Journal of Zhejiang University-SCIENCE B (Biomedicine & Biotechnology) 2021 22(8):647-663
www.jzus.zju.edu.cn; www.springer.com/journal/11585
E-mail: jzus_b@zju.edu.cn

Research Article

https://doi.org/10.1631/jzus.B2000590

Layers of interstitial fluid flow along a "slit-shaped" vascular adventitia

Hongyi LI[1,2]✉, You LYU[2], Xiaoliang CHEN[3], Bei LI[2], Qi HUA[1]✉, Fusui JI[2], Yajun YIN[4], Hua LI[5]

[1]*Cardiology Department, Xuanwu Hospital, Capital Medical University, Beijing 100053, China*
[2]*Cardiology Department, Beijing Hospital, National Center of Gerontology, Institute of Geriatric Medicine, Chinese Academy of Medical Sciences, Beijing 100730, China*
[3]*Radiology Department, China-Japan Friendship Hospital, Beijing 100029, China*
[4]*Department of Engineering Mechanics, Tsinghua University, Beijing 100084, China*
[5]*Institute of Computing Technology, Chinese Academy of Sciences, Beijing 100190, China*

Abstract: Interstitial fluid (ISF) flow through vascular adventitia has been discovered recently. However, its kinetic pattern was unclear. We used histological and topographical identification to observe ISF flow along venous vessels in rabbits. By magnetic resonance imaging (MRI) in live subjects, the inherent pathways of ISF flow from the ankle dermis through the legs, abdomen, and thorax were enhanced by paramagnetic contrast. By fluorescence stereomicroscopy and layer-by-layer dissection after the rabbits were sacrificed, the perivascular and adventitial connective tissues (PACTs) along the saphenous veins and inferior vena cava were found to be stained by sodium fluorescein from the ankle dermis, which coincided with the findings by MRI. The direction of ISF transport in a venous PACT pathway was the same as that of venous blood flow. By confocal microscopy and histological analysis, the stained PACT pathways were verified to be the fibrous connective tissues, consisting of longitudinally assembled fibers. Real-time observations by fluorescence stereomicroscopy revealed at least two types of spaces for ISF flow: one along adventitial fibers and another one between the vascular adventitia and its covering fascia. Using nanoparticles and surfactants, a PACT pathway was found to be accessible by a nanoparticle of <100 nm and contained two parts: a transport channel and an absorptive part. The calculated velocity of continuous ISF flow along fibers of the PACT pathway was 3.6–15.6 mm/s. These data revealed that a PACT pathway was a "slit-shaped" porous biomaterial, comprising a longitudinal transport channel and an absorptive part for imbibition. The use of surfactants suggested that interfacial tension might play an essential role in layers of continuous ISF flow along vascular vessels. A hypothetical "gel pump" is proposed based on interfacial tension and interactions to regulate ISF flow. These experimental findings may inspire future studies to explore the physiological and pathophysiological functions of vascular ISF or interfacial fluid flow among interstitial connective tissues throughout the body.

Key words: Vascular adventitia; Interstitial fluid; Connective tissue; Interfacial zone

1 Introduction

Vascular vessels consist of three layers: the tunica intima, tunica media, and tunica adventitia. They produce an intraluminal space used for the rapid transport of O_2, nutrients, waste products, and heat around the body. The outermost tunica adventitia, together with the surrounding perivascular/paravascular loose connective tissues, serves mainly to strengthen the blood vessel and anchor it to nearby organs, giving stability. However, increasing data show that the perivascular and adventitial connective tissues (PACTs) are also capable of transporting interstitial fluid (ISF) (Li et al., 2012, 2016, 2019).

In rabbits, ISF flow along venous adventitia was found along the lower extremity veins, inferior vena cava (IVC) of the abdomen and thorax, and into three grooves of the heart and pericardial cavity (Li et al., 2012). Both the tunica adventitia and its surrounding fibrous connective tissues participated in ISF flow along blood vessel walls (Li et al., 2012). In humans, ISF flow along blood vessels was identified to be along

✉ Hongyi LI, leehongyi@bjhmoh.cn
Qi HUA, huaqi5371@sina.com
Hongyi LI, https://orcid.org/0000-0001-5507-0039
Qi HUA, https://orcid.org/0000-0002-5115-2149

Received Sept. 26, 2020; Revision accepted Feb. 14, 2021;
Crosschecked June 12, 2021

not only venous adventitia, but also arterial adventitia (Li et al., 2016, 2019). Histologically, the vascular adventitia and its surrounding tissues are the fibrous connective tissues (Li et al., 2012, 2016, 2019). Adventitial ISF flow includes at least two types: fluid flow through the tunica adventitia and fluid flow through the perivascular/paravascular connective tissues.

Another pattern of fluid flow along blood vessels is via the perivascular space (PVS). This pathway has been noticed in the brain for centuries. The PVS was found between the outer and inner laminae of brain vessels or around fenestrated capillaries. Recently, a brain-wide perivascular pathway was identified and named as the glymphatic system. The system includes the periarterial influx of cerebrospinal fluid (CSF) into the brain interstitium, followed by the clearance of ISF along large-caliber draining veins, serving as a lymphatic-like clearing system in the brain (Rennels et al., 1985; Iliff et al., 2012). However, the glymphatic pathway is in the vicinity of the tunica adventitia of vascular conduits (Iliff et al., 2012). The relationship between glymphatic and ISF flow through a PACT pathway has not yet been elucidated.

In conventional interstitial physiology, the matrix of fibrous connective tissues is considered a fluid-filled porous/interstitial medium with a random net of internal pores/interstices. Based on the random porous matrix, adventitial ISF would flow diffusively under a pressure/concentration gradient and cannot flow longitudinally for a long distance (Levick, 1987; Wiig et al., 2003). However, our previous data revealed that the solid structure of fibrous matrices is a highly ordered fibrous framework that contains abundant oriented fibers (Li et al., 2019). Because neither the fibers nor the gel can flow, a possible transport space for the long-distance ISF flow might be an interfacial zone (or interfacial transport zone (ITZ)) between a solid phase (a fiber) and a liquid phase (the gel/liquid substance) (Li et al., 2016, 2019). When fluorescent ISF enters an ITZ along a fiber, the oriented fibers of fibrous matrices would work as a fibro-guiderail for a linear ISF flow and be fluorescently stained (Li et al., 2017, 2020). Thus, a longitudinal and linear ISF flow pathway can be identified by tracking the fluorescently stained fibers via fluorescence or confocal microscopy.

To explore the kinetic features of long-distance ISF flow along blood vessels in the body, we designed the following experiments to observe the movements of imaging tracers (paramagnetic contrast, sodium fluorescein, a solution mixed with different surfactants, and nanoparticles) to represent ISF flow through a PACT pathway in rabbits.

2 Materials and methods

2.1 Subjects

The study was conducted in Beijing, China, between January 2011 and August 2019. A total of 67 New Zealand White rabbits (male, body weight 2–3 kg; Keyu, Beijing, China) were involved, and the study protocol was approved by the animal ethics committee of the Institute of the People's Hospital of Peking University (No. 201170), Beijing, China. Anesthetic (pentobarbital (NIFDC, Beijing Bizi Biotech, Beijing, China) at 25–30 mg/(kg·h)) was administered intravenously before each of the following experiments. The tracer solution with 2% (0.02 g/mL) lidocaine (Acmec, Jizhi Biochemical, Beijing, China) was used for local anesthesia. Each subject was sacrificed via an overdose of pentobarbital.

2.2 Visualization methods of PACT pathways

2.2.1 Magnetic resonance imaging (MRI)

Five rabbits in the first group were examined by MRI scanning. Gadolinium-diethylenetriamine pentaacetic acid (Gd-DTPA; diluted to 156 mg/mL by physiological sodium saline; MedChemExpress, Quality Research, Zhuozhou, China) and fluorescein sodium (FluoNa; diluted to 10 mg/dL by physiological sodium saline; Solarbio, Borytech, Beijing, China) solutions were mixed. The mixed tracers (0.1–0.2 mL) were injected hypodermically into the ankle dermis using a 1-mL syringe (B. Braun Medical, Shanghai, China). There were arterial and venous vessels passing through beneath the ankle dermis. The imaging tracers were injected into the hypodermic tissues, but not the intravascular cavity, and represented an upstream site of the long-distance PACT pathway along blood vessels.

Imaging was performed using an Achieva 3.0T TX scanner (Philips Electronics, China). Each subject was scanned in real time 45–60 min after the hypodermic injection of Gd-DTPA. The images were obtained using a three-dimensional (3D) T1-weighted fast field echo (FFE) sequence with an eight-channel phased-array

head surface coil. Scanning parameters were adjusted to obtain a high spatial resolution. The acquisition time for each sequence was 4–6 min. The raw data were analyzed at an extended MR WorkSpace Station (Philips Electronics, China) with multiplanar reconstruction (MPR) and maximum-intensity projection (MIP) reconstructions. After the MRI scans, the rabbits were sacrificed and examined by fluorescence stereomicroscopy. The fluorescent images were compared with the images reconstructed by MIP.

2.2.2 Fluorescence stereomicroscopy

Five rabbits in the second group were examined by fluorescence stereomicroscopy. Firstly, incisions were made to form a flap revealing the femoral vein (FV) or the small saphenous vein (SSV) under the facial plane on the level of the thighs. Secondly, 0.1–0.2 mL of FluoNa water solution (diluted to 10 mg/dL by physiological sodium saline) was injected hypodermically into the same area of the ankle dermis as in the first group. Photos of the fluorescent ISF via the PACT pathways of FV or SSV were recorded in real time by stereomicroscopy (Nikon SMZ1000, Japan) or a digital camera (Canon) after the administration of FluoNa.

To elucidate the differences between ISF flow in the PACT pathways and blood flow in the intraluminal cavity of the blood vessel, extra surgical incisions were performed in five rabbits in the third group. Firstly, using ophthalmic scissors, an arch-shaped incision was made in a PACT pathway of SSV, including layers of covering fascia and parts of the tunica adventitia of the vessel. Secondly, a small branch of a main vein in the ankle was punctured by a 1-mL syringe, and 20–30 μL FluoNa water solution was added into the blood. Photos of the SSV were recorded in real time by fluorescence stereomicroscopy for a period of 3 min. Thirdly, 0.1–0.2 mL FluoNa water solution was dropped on the exposed main vein. The results were recorded for the following 60–90 min.

2.3 Observation of the PACT pathways by confocal laser scanning microscopy, scanning or transmission electron microscopy

Five rabbits from the fourth group were administered FluoNa and studied by confocal laser scanning microscopy (CLSM) or scanning electron microscopy (SEM) (Pan et al., 2019). One rabbit from the fourth group was administered physiological saline as a control. All five subjects were sacrificed 15 min after the hypodermic injection. The fluorescently stained tissues were sampled, including segments of the SSV, FV, IVC, anterior interventricular groove, posterior interventricular groove, coronary groove on the heart, and the right upper pulmonary veins. Corresponding samples were taken from the control rabbit. All samples in the second, third, and fourth groups were examined by CLSM, SEM, or transmission electron microscopy (TEM).

2.4 Histological examination of the PACT pathways

Cross-sections of the fluorescently stained PACT pathways in the second, third, and fourth groups were studied by hematoxylin and eosin (H&E) staining and the combined staining methods of van Gieson and Verhoeff iron-hematoxylin (VG+VIH) (Bio-engineering, Shanghai, China). The fluorescently stained samples were studied via an optical microscope after the immunostaining of the antibodies against CD31 (JC/70A, Abcam, MA, USA) and collagen IV (4595R, Abcam, MA, USA).

2.5 Powers of “push” and “pull” in driving fluid transport through the PACT pathway in vivo

To illustrate the driving force of fluid through the PACT pathways, an isolated segment of the PACT pathway on the SSV and FV was studied in five rabbits of the fifth group. Before the following experiments, both the distal and proximal sides of a segment of the FV or SSV were ligated by sutures to isolate the segmental PACT pathway between the distal and proximal sides of the vein from the surrounding tissues.

Firstly, both the distal end (upstream) and proximal end (downstream) of a venous vessel were ligated and the blood stopped completely. Then, 5 μL of FluoNa water solution was dropped on the middle of the ligated segment to observe the movement of FluoNa along the PACT pathway on the vein. Secondly, while untying the proximal ligation of the ligated vessel and keeping the distal end ligated, the movement of FluoNa along the PACT pathway was recorded. Thirdly, in a different vessel, while untying the distal ligation of the ligated vessel and keeping the proximal end ligated, the movement of FluoNa along the PACT pathway was recorded. During these experiments, the isolated vessel wall was kept moist by adding drops of physiological

saline. Fluid flow through the segmental PACTs was recorded by fluorescence stereomicroscopy.

2.6 Fluid transport through the PACT pathways in dead rabbits by mechanical manipulation of the heart

Five rabbits in the sixth group were sacrificed by an injection of 20 mL air via the auricular veins. Six hours after the sacrifice, all five rabbits were prepared as follows. Firstly, a 10-cm-long segment of the left SSV was exposed to air in all five subjects. Secondly, two rabbits were selected and 50 μL of collagenase type I solution (diluted to 0.1 g/mL by physiological saline) was administered in the proximal end of the left SSV. Thirdly, the thoracic cavities of all five sacrificed rabbits were opened, and then the heart apexes were cut open to ensure the right and left ventricular chambers to be exposed to air.

After the above preparation, 0.1 mL of FluoNa water solution was injected hypodermically into the ankle dermis of the exposed left SSVs. Without extra manipulation, the movement of FluoNa along the PACT pathways was observed for 60 min. The exposed heart was then compressed repeatedly according to the standard procedure of open-chest cardiac compression at a frequency of 60–80 beats/min for 20 min. The movement of the FluoNa was continuously photographed by stereomicroscopy. The fluorescently stained PACTs sampled from the left SSV, the IVC in the splanchnocoele, the coronary groove, and the anterior and posterior ventricular grooves were also studied by CLSM.

2.7 Examination of the transport of nanoparticles of various sizes through the PACT pathways in live rabbits

We used two types of nanoparticles of different sizes to observe whether they could be transported via the PACT pathways in live rabbits. Gold nanoparticles were used in five rabbits of the seventh group and fluorescent polystyrene (PS) spheres in five rabbits of the eighth group. A 10-cm-long segment of the PACT pathway of both the left and right SSVs was exposed to air in each rabbit of the seventh and eighth groups.

In the seventh group, 10 μL phosphate-buffered saline (PBS) solution mixed with five types of colloidal gold nanoparticles (5, 10, 20, 40, or 60 nm in diameter) was dropped into the distal end of the PACT pathways in each subject. The proximal end of the SSV was sampled 10 min after administration and subsequently examined by TEM.

In the eighth group, 10 μL PBS solution mixed with two types of fluorescent PS spheres (30 or 100 nm in diameter) was dropped into the distal end of the PACT pathways in each subject. The movement of the fluorescent PS spheres through the exposed SSV was recorded by fluorescence stereomicroscopy.

2.8 Observation of the movement of a mixed solution of FluoNa and surfactant through the PACT pathways

Five rabbits in the ninth group were studied to observe the movement of a mixed solution of FluoNa and a surfactant. The mixed solution was a water solution of FluoNa (diluted to 156 mg/mL by physiological saline) and an anionic surfactant, sodium dodecyl sulfate (SDS; diluted to 104.00 mmol/L by physiological saline at 25 °C; Borytech). A 10-cm-long segment of the PACT pathway of both the SSV and FV was exposed to air in each rabbit of the ninth group.

Mixed tracers (0.1–0.2 mL) were injected hypodermically into the ankle dermis of each subject. The movements of the mixed tracers through the PACT pathways of the exposed FV or SSV were recorded in real time by fluorescence stereomicroscopy in all five rabbits.

2.9 Observation of the movements of other nonionic and cationic surfactants through the PACT pathways

To observe the effects of different types of surfactants on the movement of FluoNa through the PACT pathways, the other ten rabbits were divided equally into the tenth and eleventh groups. The surfactants were the nonionic surfactant, Trixon-100, and the cationic surfactant, hexadecyltrimethylammonium bromide (CTAB). Each type of surfactant was tested in five rabbits of each group. The concentrations were 27.60 mmol/L Trixon-100 and 7.20 mmol/L CTAB (diluted by physiological sodium solution at 25 °C; Acmec, Jizhi Biochemical, Beijing, China). The concentration of each solution was six times the critical micelle concentration of each surfactant at 25 °C. The experimental procedures were the same as those for SDS in the

ninth group (Section 2.8). The movement of each fluorescent surfactant solution through the PACT pathways of the exposed FV or SSV was photographed during real-time observation by fluorescence stereomicroscopy.

2.10 Comparison of the pericardial fluid following injection of physiological saline solution or SDS solution by echocardiography

In three rabbits of the twelfth group, a total of 3–4 mL FluoNa water solution was injected hypodermically into the ankle dermis (including the left and right sides) of each rabbit, as described previously (Li et al., 2012). In three rabbits of the thirteenth group, a total of 3–4 mL FluoNa SDS solution was injected hypodermically into the ankle dermis (including the left and right sides) of each rabbit. Immediately afterwards, the pericardial fluid of each subject was detected in real time by echocardiography. After echocardiography, the rabbits were sacrificed and their thoracic cavities were opened to examine the amount of pericardial fluid.

2.11 Observation of the movement of ISF through the PACT pathways under high concentrations of SDS solution

To observe whether ISF transport through the PACT pathways could be interrupted by high concentrations of SDS solution, six rabbits in the fourteenth group were studied. SDS solutions, diluted to 5%, 10%, or 20% (1%=0.01 g/mL) in physiological saline, were prepared and each solution was administered to a pair of subjects. The FV of each subject was exposed by surgery and bathed in SDS solution while the rabbits adopted a supine position. A total of 0.1–0.2 mL FluoNa water solution was injected hypodermically into the ankle dermis. The FluoNa transport processes via the PACT pathway along the FV in different SDS solutions were recorded by real-time fluorescence microscopy.

3 Results and discussion

The kinetics of ISF flow along vascular vessels needs to be further clarified by comparison with our previous studies (Li et al., 2012, 2016, 2019, 2020). Because of the lack of a direct imaging technique and the complexities of multiscale measurements of fluid flow in fibrous connective tissues, we used multiscale and topographical approaches to explore ISF flow through a venous PACT pathway in rabbits.

3.1 Systemic PACT pathways of ISF flow in the body visualized by MRI and fluorescence stereomicroscopy

In the first group, visualization of the systemic distributions of the long-distance PACT pathways revealed by MRI was clearly enhanced by paramagnetic Gd-DTPA at the macroscopic level. These pathways included the SSV and FV in the lower limbs, the IVC of the abdominal and thoracic cavities, and some tissues of the heart (Figs. 1a and 1b; Video S1). However, the current MRI technique could not identify whether the Gd-DTPA was inside or outside the blood or lymphatic vessels. Tracing the FluoNa-stained tissues under a fluorescence stereomicroscope in the second group showed that the fluorescein had stained the tunica adventitia enhanced by MRI, and the surrounding tissues of venous vessels other than lymphatic vessels (Figs. 1c, 1f, and 1i). When the thoracic cavity was opened, the coronary, anterior and posterior grooves of the heart were clearly stained by the fluorescein from the PACT pathways. By histological analysis and CLSM, the intrinsic structures of the PACT pathways were identified as the outermost fibrous connective tissues covering the vessels from the extremities into the heart. These tissues contained longitudinally assembled and cross-linked fibers (Figs. 1d, 1e, 1g, 1h, and 1j–1n). Samples of the PACT pathways were examined by TEM and SEM to confirm the presence of cross-linked fibers at a micrometer scale (Figs. 1o and 1p). These findings coincided with our previous findings (Li et al., 2012, 2016, 2019).

As extracellular tracers, both Gd-DTPA and FluoNa can enter blood and lymphatic vascular vessels. In this and our previous studies (Li et al., 2012), it was observed clearly that FluoNa had not only entered the blood circulation via capillaries and lymphatics, but also stained the tunica adventitia of the veins from the limbs to the heart. There are no anatomical or histological records of lymphatic vessels distributed inside tunica adventitia along the entire vascular vessels. In our previous studies (Li et al., 2012), the lymphatic vessels were visualized by a lymphotropic tracer (a large-molecular weight fluorescein 5-isothiocyanate (FITC)-dextran) in the vicinity of venous vessels, but not inside the tunica adventitia. Histological analyses of CD31 and collagen (Col) IV (Figs. 1l and 1m) showed no ring-like structures distributed in venous adventitia of the veins from the limbs to the heart. Thus, the pathways enhanced by

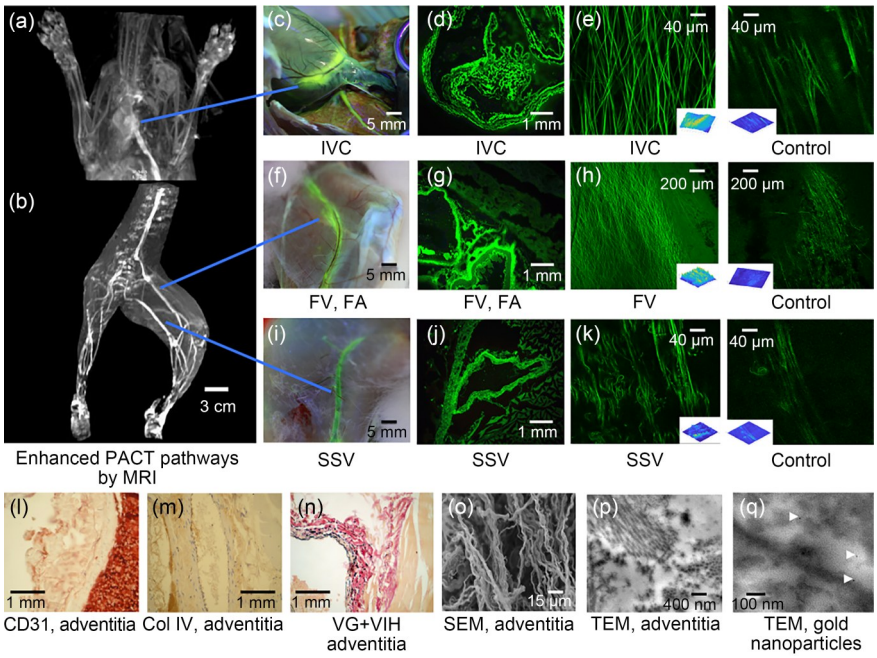

Fig. 1 Perivascular and adventitial connective tissue (PACT) pathways. (a, b) A panorama of the enhanced long-distance PACT pathways originating from the ankle dermis in the first group by magnetic resonance imaging (MRI). (c) Segments of inferior vena cava (IVC), coronary groove, and pulmonary veins were stained by fluorescein sodium (FluoNa) from the ankle dermis in the second group. (d) A cross-sectional view of a sample from (c) by frozen microscopy showed that the vessel wall and a venous valve were stained. (e) Abundant fluorescently stained and cross-linked fibers in venous adventitia were revealed by confocal laser scanning microscopy (CLSM), which were running longitudinally toward the long axis of the vein and sampled from (c). (f) Segments of the femoral vein (FV) and femoral artery (FA) were stained by FluoNa from the ankle dermis in the second group. (g) A cross-sectional view of (f) showed that the venous and arterial adventitia and their surrounding tissues were stained. (h) Fluorescently stained fibers in the venous adventitia of (f) were revealed by CLSM. (i) A segment of the small saphenous vein (SSV) was stained by FluoNa from the ankle dermis. (j) A cross-sectional view of (i) showed that the venous adventitia and its surrounding tissues were stained. (k) Fluorescently stained fibers in the venous adventitia of (i) were revealed by CLSM. (l) (×40, CD31) and (m) (×20, collagen IV (Col IV)) showed that no numerous ring-like groupings or linear structures within the venous adventitia and its surrounding loose connective tissues were revealed by immunohistochemical staining. (n) The tunica adventitia of the stained vein was composed of abundant collagenous fibers (red) and elastic fibers (black) by van Gieson and Verhoeff iron-hematoxylin (VG+VIH) staining method. (o) Scanning electron microscopy (SEM) and (p) transmission electron microscopy (TEM) showed that the venous adventitia contained abundant fibers. (q) Gold nanoparticles of 5-, 10-, and 20-nm diameters were located among the fibril bundles (white arrows) of the downstream PACT pathway in the seventh group.

Gd-DTPA and those stained by fluorescein in this study were the PACT pathways.

3.2 Difference between ISF flow through the PACT pathways and blood flow through the intraluminal cavity

To illustrate the differences between ISF flow in a PACT pathway and intraluminal blood flow, two types of angiography were used. Firstly, in the third group a segment of FV was exposed and an incision was made in the PACT pathway. When 20–30 μL FluoNa solution entered and mixed with blood in a branch of the saphenous veins, the intravascular blood was partially stained by the fluorescein. A spiraled and rotated flow pattern of blood flow was observed inside the lumen (Video S2). However, the incision of the PACT pathway showed no staining at that time.

Secondly, after a fluorescent longitudinal channel in the PACT pathway was clearly displayed in the ninth group (Figs. 2a and 2b), 2 mL FluoNa solution was injected via the ear vein in two subjects. The intraluminal FluoNa visualized the blood in the femoral artery (Fig. 2c) and FV (Fig. 2d). The calculated velocity of the venous blood was 4–6 cm/s, which was similar to 6–7 cm/s found in previous studies (Qian et al., 2010).

Thus, the demonstrated ISF flow through a PACT pathway was clearly distinguished from arterial and venous blood flows. Moreover, blood flow through a

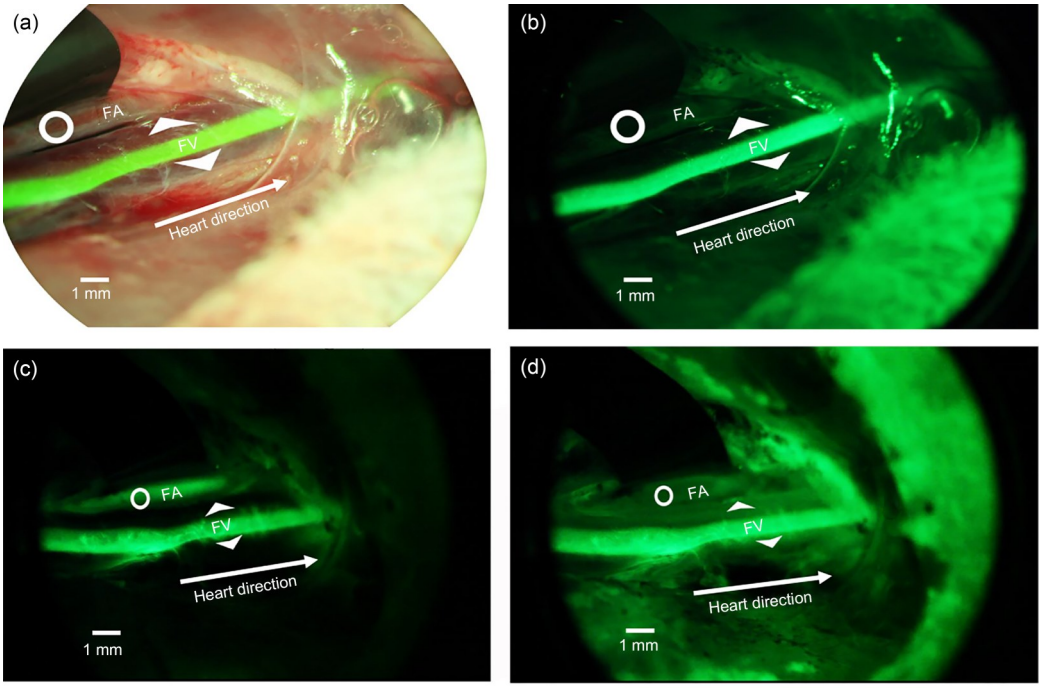

Fig. 2 Differences between fluorescein sodium (FluoNa) flow through the perivascular and adventitial connective tissue (PACT) pathway and intravascular cavity. (a) A longitudinal transport channel in the PACT pathway of the femoral vein (FV) stained by FluoNa sodium dodecyl sulfate (SDS) solution, from the ankle dermis in the ninth group (merged dark-field and bright-field images). The diameter of the stained PACT pathway was smaller than that of the vein (indicated by two white arrows). (b) The dark-field image of (a). (c) The femoral arterial blood (femoral artery (FA), indicated by a white circle) stained at 6 s after intravascular injection of FluoNa into the ear vein. (d) Both the femoral arterial blood and venous blood were stained by intravascular FluoNa, while the longitudinal transport channel in the PACT pathway was clearly stained on the venous adventitia of the femoral vein. Thus, ISF flow through a PACT pathway was distinguishable from arterial and venous blood flow.

vascular conduit is considered a laminar flow at low velocity, laminar-turbulent transitional flow, and a turbulent flow at high velocity. Our data suggested that the outermost layer of the blood flow column was spiraling and rotating inside the vascular conduit like a bullet fired through a gun-barrel with a periodic internal spiral ridge. One flow circle of spiraling and rotating blood inside a vascular vessel was found to be 1.3–1.9 s. The flow length of one circle was calculated to be 5.2–11.4 cm, given a speed of 4–6 cm/s and a diameter of 2 mm of the femoral venous blood flow (Video S2). We predicted that there would be a periodic internal spiral ridge-like structure in the tunica intima of vascular vessels. Further studies are needed to verify this.

3.3 ISF flow speed through the PACT pathways calculated from fluorescence stereomicroscopy

To estimate the velocity of ISF flow through a PACT pathway, in the second group the FluoNa flow was recorded by real-time fluorescence stereomicroscopy. During initial observation, it was too difficult to catch the front end of the FluoNa flow along the vessels by stereomicroscopy. Fortunately, many fluorescent spots could be found to emerge and move along the PACT pathways during a 50–60-min observation when the gross fluorescence intensity began to differentially decrease (Video S3). After 60–70 min of observation, we found that a few large clumps of fluorescein were continuously flushed away along the vessels as well (Video S4). The calculated speed of FluoNa spots was 3.6–15.6 mm/s and their size was around 10–20 μm (Figs. 3a and 3b). The calculated speed of FluoNa clumps was 0.1–7.6 mm/s and their size was around 50–400 μm (Figs. 3c and 3d).

3.4 Layers of ISF flow in a PACT pathway

To identify in which part of the tunica adventitia and perivascular tissues for ISF flow occurred along the vessel, in the third group an incision was made in a PACT pathway of the SSV. The cutting plane of the

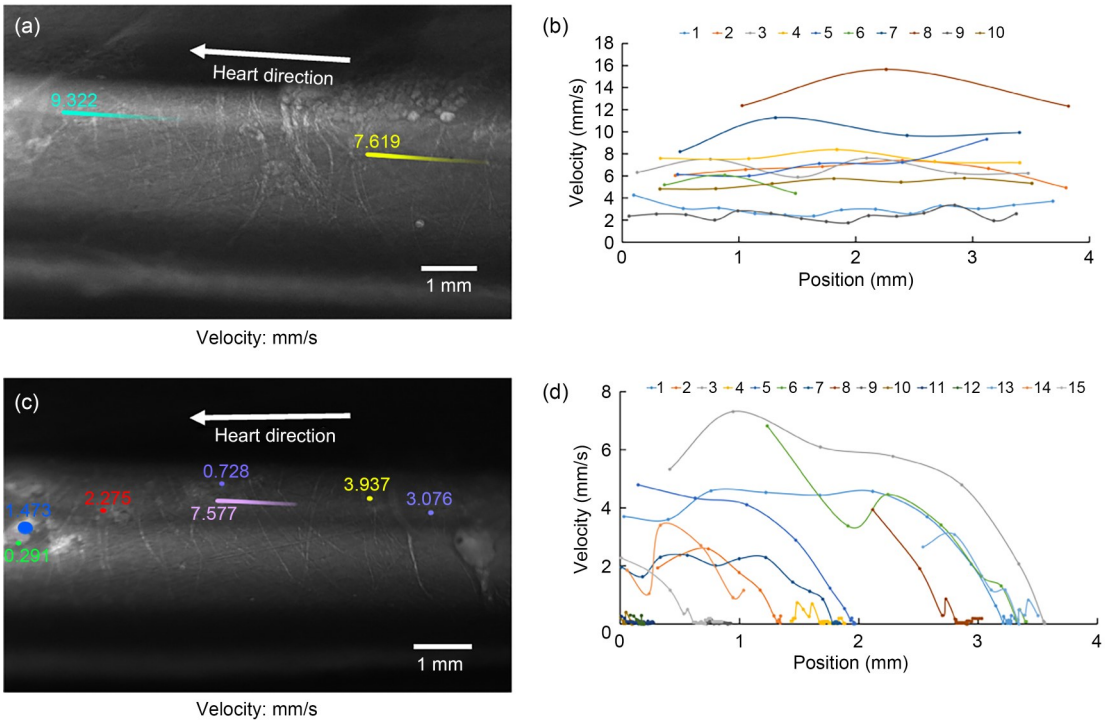

Fig. 3 Velocity of a few fluorescein sodium (FluoNa) spots or clumps flowing along adventitia. (a) Flow trajectories of two FluoNa spots along a segment of the perivascular and adventitial connective tissue (PACT) pathway during a 50–60-min observation (Video S3). After 60–70 min of observation, a few large FluoNa clumps were continuously flushed away along the vessels (c). (b) The velocity of a total of ten FluoNa spots and their flow trajectories along the adventitia. The calculated speed of FluoNa spots was 3.6–15.6 mm/s and their size was about 10–20 μm, which might represent fluid flow along adventitial fibers. (c) The trajectories of seven FluoNa clumps flowing along adventitia (Video S4). (d) The velocity of a total of 15 FluoNa clumps and their flow trajectories along the adventitia. The calculated speed of the clumps was 0.1–7.6 mm/s and their size was about 50–400 μm, which might represent fluid flow in the space between the tunica adventitia and its covering fascia.

arch-shaped incision by scissors included layers of the fascia covering on tunica adventitia (Figs. 4a and 4b). When 0.2 mL FluoNa solution was injected hypodermically into the ankle dermis which represented an upstream site of the PACT pathway, continuous ISF flow along the cutting plane was visualized to have stained the PACT pathway step-by-step (Figs. 4c–4f). The successive staining process showed that firstly, ISF flowed continuously through the tunica adventitia, and secondly, crossed layers of fascia and into the surrounding connective tissues (Figs. 4g–4j). When more fluorescent fluid was injected into the ankle dermis, the fluorescent ISF flowed and emerged out continuously along the arch-shaped incision (Video S5). Then, it was clearly showed that a constant bulk-like flow through the space between the adventitia and the covering fascia (Video S6). Thus, there were at least two layers of the continuous ISF flow in the PACT pathway (Fig. 4k): (1) ISF flow between the covering fascia and adventitia; (2) ISF flow through adventitia. The direction of ISF flow through venous PACT pathways was toward the heart. Usually, the covering fascia and perivascular connective tissues contain several layers of fascia. Fluid flow in the perivascular spaces of the brain is probably a part of the layers of ISF flow along the adventitia of the vasculature around the body.

During the early stage of ISF flow along the adventitia under the covering fascia, small FluoNa spots were clearly found to flow down along the adventitia (Fig. 4c, Video S3). During the late stage of ISF flow when sufficient fluid added, large FluoNa clumps were found to flow down along the edge of the arch-shaped incision and the space between the adventitia and its covering fascia (Video S6). Thus, the FluoNa spots might represent fluid flow via a smaller space along adventitial fibers, and the FluoNa clumps might represent fluid flow via a bigger space between the adventitia and its covering fascia. The PACT pathways

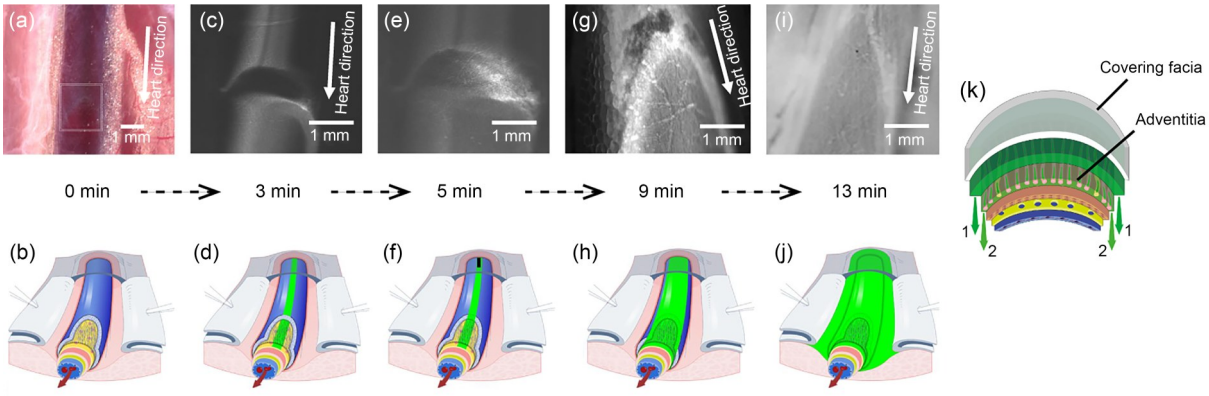

Fig. 4 Successive processes of interstitial fluid (ISF) flow through the perivascular and adventitial connective tissue (PACT) pathway. (a) An arch-shaped incision of fascia covering on the tunica adventitia of a venous vessel (white box). Partial tunica adventitia was exposed. (b) A diagram of (a). (c, d) After hypodermic injection into the ankle dermis, fluorescein sodium (FluoNa) flowed along the PACT pathway on the vein and stained the adventitia firstly, but the arch-shaped incision was not stained. (e, f) The arch-shaped incision was gradually stained by FluoNa secondly. (g, h) Both the adventitia and the incision of the covering fascia were stained thirdly. (i, j) When sufficient fluid come into the PACT pathways, the entire tunica adventitia and perivascular tissues were stained. (k) There were at least two layers of the continuous ISF flow in a PACT pathway: 1. ISF flow between the covering fascia and adventitia; 2. ISF flow through adventitia.

comprised at least two types of the continuous ISF flow in physiological conditions. In the perivascular connective tissues, more types of the continuous ISF flow in layers of fascia need to be identified.

3.5 Two types of driving forces for ISF flow in a PACT pathway: "pull and push"

The force driving the flow of fluid through a PACT pathway needs to be identified. To observe the driving force of ISF flow, fluid movements along the PACT pathway were studied in a segment of a vein that was isolated by sutures from the surrounding tissues and exposed to air. "Push and pull" experiments revealed at least two types of in vivo forces driving ISF flow (Figs. 5a–5h). Without either of these two forces, the fluorescein would simply diffuse around the original drop site (Figs. 5b and 5f). By either "push" or "pull," the fluorescein in the middle of the isolated segment was driven centripetally and stained the downstream PACT pathway (Figs. 5d and 5h). Because the segmental vessel was exposed to air, interstitial pressure might not have been generating the "push" or "pull" force. Limited by the instantaneous measurements of interstitial pressure, an alternative method was performed.

In five sacrificed rabbits of the sixth group, the right and left ventricular apexes were cut off and then the ventricular chambers were opened to the air. The interstitial pressure in the PACT pathways, blood pressure, and blood flow inside the vessels vanished. By repeated cardiac compression on the right and left ventricular chambers, FluoNa in ankle dermis was "pulled" centripetally and stained the tunica adventitia of the SSV, IVC, and the anterior groove of the heart in the three rabbits with intact PACT pathways. When the fibrous framework on the SSV was destroyed by collagenase type I, FluoNa from the ankle only was diffused in the injection site and could not be "pulled" by cardiac compression in the other two subjects. Therefore, to "pull" ISF from the long-distance PACT pathways might depend on at least two factors: the mechanical heart beatings as a driving source and long-distance PACT pathways containing an intact fibrous framework. These results coincided with those of our previous studies of amputated lower legs and cadavers (Li et al., 2016, 2019). The "push" force might be due to sufficient supplies of ISF from the upstream PACT pathway, which is generated from capillaries. Examination of cadavers showed that the structural framework of the vasculature's adventitia is composed of micron-sized fibers longitudinally assembled from the distal veins to the epicardium, working as a guide-rail for a long-distance ISF flow (Li et al., 2019). Herein, the kinetic and dynamic patterns of ISF flow found in a PACT pathway toward an active dynamic driving source are unique in biological and living systems and need to be comprehensively studied in the near future.

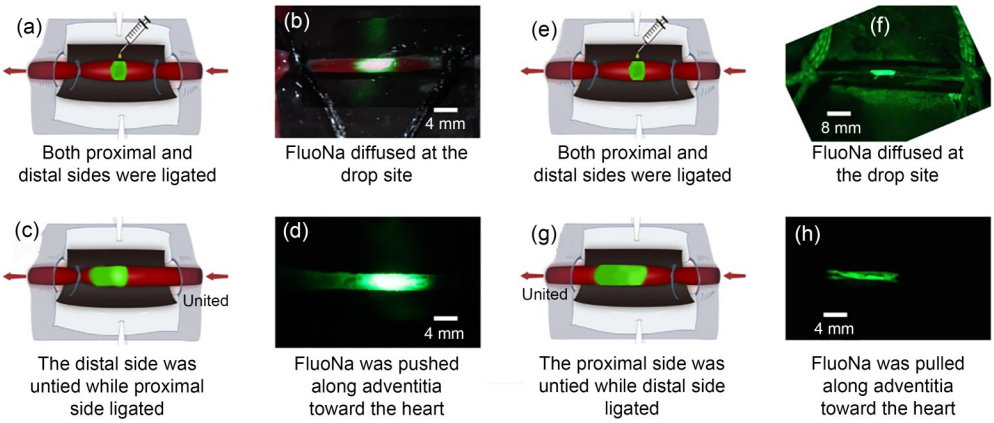

Fig. 5 Two types of driving force to "push and pull" ISF flow in a perivascular and adventitial connective tissue (PACT) pathway. (a, e) A segment of venous vessel with ligated sutures on the proximal and distal sides. (b, f) Interstitial fluid (FluoNa) in the middle of the ligated segment diffused locally at the drop site when both the proximal and distal sides were ligated. (c, d) FluoNa was "pushed" by the force from the distal side when the distal side was untied. (g, h) FluoNa was "pulled" by the force from the proximal side when the proximal side was untied. Without these two forces, FluoNa would simply diffuse around the original drop site. By either the "push" or the "pull," the fluorescein in the middle of the isolated segment would be driven centripetally and stain the downstream PACT pathway.

3.6 Estimated pore sizes in a PACT pathway for ISF flow

In conventional physiology, a fibrous matrix can be considered a porous medium. The composition of PACT pathways is mainly fibrous matrix. Therefore, porous PACT pathways may have two types of pores: closed and connected accessible to flow (Tokunaga and Wan, 1997; Tuller et al., 1999). As revealed by CLSM, the stained long-distance PACT pathways were composed of abundant fluorescently stained fibers along the venous vessels of the lower limbs, IVC and into the anterior groove of the heart. In the controlled subject of the fourth group, there were no signs of fluorescently stained fibers in the PACT pathways along the veins into the heart. Thus, the stained fibers of the PACT pathways were the results of fluorescent ISF flow through the long-distance pathways. Because neither the fibers nor the gel-like matrix can flow, the transport space in the PACT pathways might be the topologically connected ITZs along the fibers. In the context of a porous medium, the longitudinally connected ITZs through the PACT pathways were equivalent to the connected pores or pore throats for fluid flow.

To determine the pore size of the longitudinally connected ITZs under physiological conditions, in the seventh and eighth groups we explored the permeabilities of two types of nanoparticles through the PACT pathways. Following administration into the upstream pathways, the 5-, 10-, and 20-nm gold nanoparticles and the 30-nm PS microspheres were found in the downstream PACT pathways by TEM (Fig. 1q) and by real-time fluorescence stereomicroscopy. The 40- and 60-nm gold nanoparticles or 100-nm PS microspheres were not detected there. Thus, the in vivo pore size of the connected ITZs along the fiber might be under 100 nm and accessible for a nanoparticle of about 10–20 nm, which coincides with our previous findings in human cadavers (Li et al., 2019).

Given the understandings of interfacial science, fluid transport through such a nanoscale interfacial zone with diameters ranging from 10 to 100 nm would be enhanced by interfacial effects and interactions. Such transport would differ significantly from blood or lymph transport through macroscale vascular conduits by pressure gradients, as well as diffusive transport (Chen et al., 2008; Whitby et al., 2008). In addition, the PACT pathways were composed of abundant collagenous fibers, combined with a few elastic fibers (Fig. 1n). Typically, the collagenous molecules were hydrophilic and rich in the amino acid sequences of glycine-proline-X and glycine-X-hydroxyproline. The hydrophobic elastic fibers were rich in glycine and proline. Thus, the surfaces on the fibril bundles must contain both hydrophilicity and hydrophobicity to some extent (van Oss, 2007). Here, we postulated that fluid transport through the PACT pathways would be

impacted by a surfactant due to the potential hydrophobic and hydrophilic characteristics of the connected ITZs in such pathways (Khan, 1996; Holmes, 1998; Holmberg et al., 2003).

3.7 Two parts in a PACT pathway: a longitudinal transport channel and an absorptive part

In the second group, the dynamic transport processes of ISF flow along blood vessels indicated that there were two parts in a PACT pathway: a longitudinal transport channel along the vascular vessel and an absorptive part around the tunica adventitia. In the ninth group, the two parts of the PACT pathway were visualized by FluoNa SDS solution (Figs. 6d–6f). During the first 15–20 min of observation, the imaging mixture of FluoNa SDS solution stained 2–3 transport channels along the FV and one transport channel along the SSV. These longitudinal transport channels had a clear boundary and the absorptive part of the PACT pathways was not then stained. After about 25–40 min, the absorptive part of either FV or SSV was gradually stained by the fluorescein from the transport channel. Sixty minutes after administration, the PACT pathways surrounding the vessels were totally stained, like those in the second group (Figs. 6a–6c). Following CLSM, the PACT pathways in the ninth group appeared full of fluorescently stained fibers.

The same results were found following administration of a nonionic surfactant, Trixon-100, in the tenth group. Following administration of a cationic surfactant

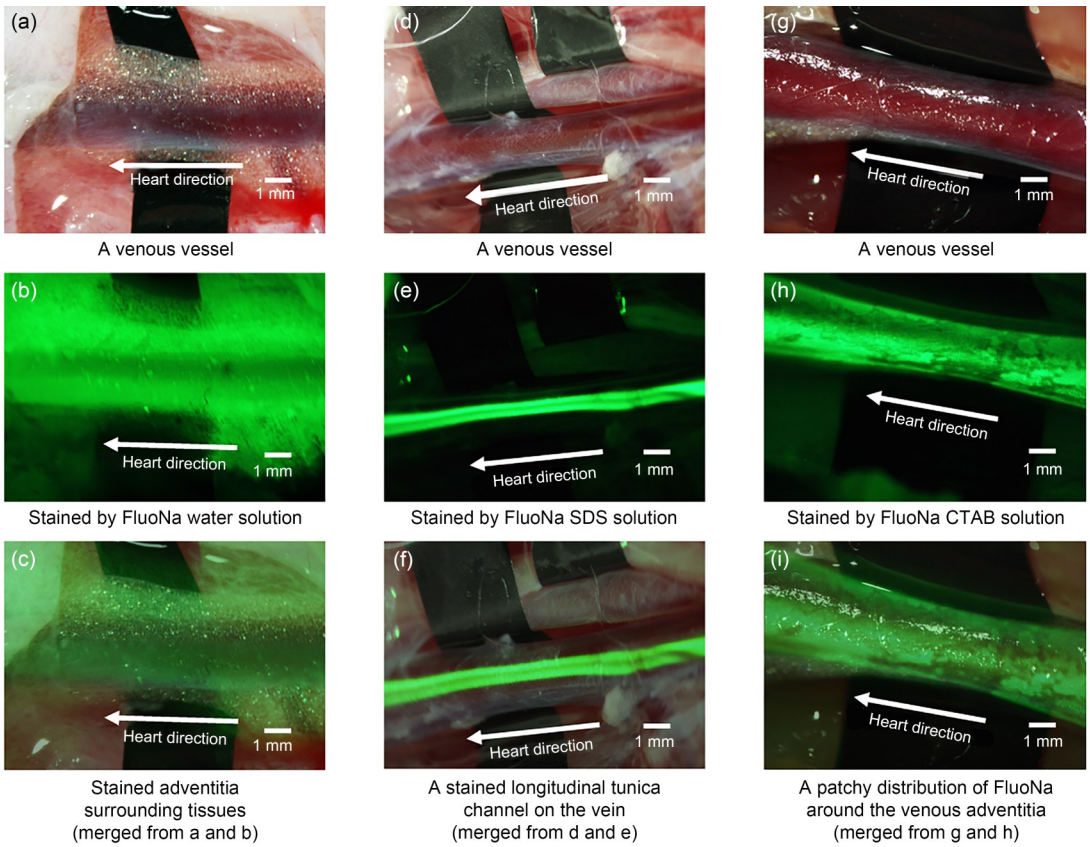

Fig. 6 Two types of interstitial fluid (ISF) flow through a perivascular and adventitial connective tissue (PACT) pathway demonstrated by interstitial fluid (FluoNa) surfactant solution. (a–c) At 10 min after the injection of 0.1 mL FluoNa water solution into the ankle dermis, the entire tunica adventitia surrounding the vein was stained. (d–f) At 10 min after injection of either 0.1 mL FluoNa sodium dodecyl sulfate (SDS, anionic surfactant) solution or 0.1 mL FluoNa Trixon-100 (nonionic surfactant) solution into the ankle dermis, a longitudinal transport channel was clearly visualized within the PACT pathway of venous vessels. Usually, there were 2–3 transport channels in the PACT pathway of the femoral vein (FV) and one transport channel on the small saphenous vein (SSV). (g–i) At 10 min after the injection of 0.1 mL FluoNa hexadecyltrimethylammonium bromide (CTAB, cationic surfactant) solution into the ankle dermis, a patchy distribution of FluoNa around the entire PACT pathway on the venous vessel was observed.

in the eleventh group, the longitudinal transport channel along the PACT pathways was visualized by CTAB, but with a fuzzy boundary (Figs. 6g–6i). When the transport channel was visualized, the absorptive part began to stain gradually, but unevenly. At 15–20 min after administration, the PACT pathways surrounding the FV and SSV showed a patchy distribution of fluorescein (Figs. 6h and 6i). Following CLSM, the PACT pathways in the ninth, tenth, and eleventh groups were also full of the fluorescently stained fibers.

The macroscopic behavior of adventitial ISF flow supports the existence of two parts in a PACT pathway: a longitudinal transport channel and an absorptive part, like a fractured-porous rock that contains highly ordered polygonal pores connected to slit-shaped spaces or pore-throats (Tokunaga and Wan, 1997; Tuller et al., 1999; van Oss, 2007). The transport channel was similar to a pore throat, accessible for fluid transport through a porous medium. The absorptive part was equivalent to the closed pores that attract free water into a porous medium. The transport channel might be related to the stained ITZs along the longitudinally assembled fibers, because neither the fibers nor the tissue gel can flow (Li et al., 2020). The absorptive part might be associated with the gel-like ground substances of the adventitial matrix, which is a highly absorbent biological gel (Levick, 1987).

Surfactants are the compounds that lower surface or interfacial tension between two phases (Khan, 1996; Holmes, 1998; Holmberg et al., 2003; van Oss, 2007). We speculated that when mixed with a surfactant, the interfacial tension of fluid in contact with the gel would be lowered and the absorption of the fluorescent ISF into the gel would be suspended. In the ninth and tenth groups with the anionic or nonionic surfactants, the transport of fluorescent ISF into the absorptive part was significantly delayed (Figs. 6d–6f). However, in the eleventh group with cationic surfactant, the transport of fluorescent ISF into the absorptive part had not completely stopped (Figs. 6g–6i). This may have been because the positively charged cationic surfactants were attracted by the negatively charged gel of the adventitial matrix thereby weakening their ability to block the movement of fluorescent ISF into the absorptive part (Levick, 1987; Wiig et al., 2005), which resulted in the patchy appearance around the adventitia. By contrast, the anionic and nonionic surfactants have a negative or neutral charge and would be repulsive to the negatively charged gel of the adventitial matrix, which resulted in the totally suspending of the diffusion from the transport channels into the surrounding gel.

3.8 ISF flow through a longitudinal transport channel in a PACT pathway

To explore ISF flow through a longitudinal transport channel in a PACT pathway, two types of experiments were performed. Firstly, the peripheral ISF via the PACT pathways into the pericardial cavity was examined following injection of FluoNa water solution or FluoNa SDS solution. In the twelfth group with hypodermic injection of 3–4 mL FluoNa water solution, extra pericardial fluid was found by echocardiography in about 40–60 min. In the thirteenth group, following hypodermic injection of 3–4 mL FluoNa SDS solution (containing 0.05 g/mL SDS), there was no sign of pericardial effusion. The amount of ISF flow through both the transport channel and the absorptive part of the PACT pathways was significantly reduced by the surfactant.

Secondly, in the fourteenth group, the ISF flow through a PACT pathway was tested by injection of 0.05, 0.10, or 0.20 g/mL SDS solution. Increased surfactant concentration was associated with reduced ISF transport through the PACT pathway, which was finally suspended in the 0.20 g/mL SDS solution. Although studies on the detailed mechanisms are needed, these findings strongly suggest the involvement of interfacial interactions in ISF flow through the transport channel and absorptive part of a PACT pathway of the vasculature (Tuller et al., 1999).

3.9 A working hypothesis for ISF dynamic transport

Based on the current data and our previous findings on the periodic to-and-fro “gel pump,” the dynamotaxis, and longitudinally assembled and topologically connected ITZs through fibrous connective tissues (Li et al., 2017, 2019, 2020), a working hypothesis for the ISF dynamic transport mechanism was proposed. (1) Connective tissues provide the gel-like ground substances to create an interfacial zone paving on a solid surface everywhere in the body, such as a fiber, a cell, a bundle of fibers, a group of cells, layers of fascia, and other solid surfaces. The interfacial zones are a multiscale, multilayer, and multiform space ranging

from nano-micron-sized thickness to meter-sized length in biological systems. (2) ISF flow through a network of interstitial connective tissues depends on two essential factors: a "gel pump" and an ISF flow pathway, the two parts of which are topologically connected via the interconnected ITZs. When fluid comes into the ITZs, a long-distance fluid film is formed continuously from the pathways into the pump. (3) The "gel pump" is the gel-like fibrous matrices of connective tissues in a driving source or center, working as a device that drives fluids by mechanical action. When a tissue or an organ is compressed and decompressed repeatedly, the gel-like matrix in the driving source or center becomes a "drive pump," named as "gel pump," by attracting fluid into the gel-like matrix and releasing it into the surrounding cavity. (4) When fluid in the gel pump flows out, fluid would be resupplied from the neighboring ISF flow pathways via the topologically interconnected ITZs within them. Consequently, fluid in the neighboring ISF flow pathway would be resupplied from the distal ISF flow pathway via the topologically interconnected ITZs between them as well. When the gel pump is compressed and decompressed repeatedly by to-and-fro mechanical movements, fluid at a far distance would be conveyed by the long-distance ISF flow pathways into the "gel pump" via the long-distance interconnected ITZs and extra fluid would be "pumped" into the sac of the driving source or center as well as the spaces surrounding the long-distance ISF flow pathways. (5) Within the long-distance and topologically connected ITZs from the ISF flow pathways into the gel pump, the interfacial interactions of fluid films with the solid surfaces and the contacting gel might be a dominating driving force to drive fluid flow as well as to absorb fluid into the gel (Ziemys et al., 2012). (6) Theoretically, the absorptive processes of fluid into the gel via the ITZs would be more efficient than the diffusive processes of fluid into the gel without the help of an ITZ. When the gel is compressed, fluid would be squeezed out of the gel into the surrounding environments rather than into the ITZs. When the gel is decompressed, fluid in the ITZs would be absorbed easily into the gel and resupplied by the fluid from a neighboring ITZ. In another word, the "gel pump" of the fibrous connective tissues is a one-way valve that normally allows fluid to flow from the ITZs into the gel, meanwhile, to prevent the fluid from the gel into ITZs, when the repeated to-and-for mechanical forces are performed. The hypothetical "gel pump" or "gel driver" for dynamic mechanism to regulate ISF flow needs further verifications.

In the human cadaver experiments, the peripheral ISF in the thumb was driven into the superficial tissues on the heart which was repeatedly compressed by an automatic cardiac compressor (Li et al., 2019). In live rabbits, peripheral ISF was conveyed by a PACT pathway into the tissues on the heart and entered the pericardial cavity, causing pericardial effusion (Li et al., 2012). In the surfactant study, we found that the long-distance transport processes of ISF in a PACT pathway were suspended by 20% SDS solution. Presumably, the interfacial interactions of fluid with the solid surfaces and the contacting gel in the long-distance ISF flow pathways were damaged by the increasing amount of surfactant. However, the exact dynamic mechanisms of interfacial interactions for ISF flow need further study.

3.10 ISF in the PACT pathways converged into capillaries and nearby venous vessels

As to the relationship with blood circulation, we found that the fluorescent ISF in a PACT pathway was retaken by the capillaries into nearby venous vessels (Figs. 7a–7c, Video S7). The results coincided with the understanding of ISF exchange with capillaries described by the Starling equation (Aukland and Reed, 1993; Hall and Guyton, 2011). Thus, the continuous ISF flow in a PACT pathway can exchange constantly with blood circulation via the capillaries along the PACT pathways of the systemic and pulmonary circulations, including the coronary circulation. Interestingly, if the adventitial ISF flows along all vascular vessels of the vasculature into the epicardium of the heart, will the coronary capillary network retake adventitial ISF totally or partially back into the coronary veins? Otherwise, does adventitial ISF from the systemic circulation circulate partially round the pulmonary circulation?

3.11 Respiratory movement of the lungs was another potential driving center for ISF flow

In the fourth group, CLSM showed that the FluoNa from the legs stained the covering fascia on the lungs

and the PACT pathways of the pulmonary vein were also composed of longitudinally assembled and cross-linked fibers (Fig. 8). The ISF flow direction in the PACT pathway on the pulmonary vein was found toward the heart in a subject of the fourth group (Fig. 9). Thus, respiratory movements seemed to be another driving center to "pull" the ISF from the PACT pathways of the legs. In the pulmonary circulation, whether the adventitial ISF will flow along the pulmonary arteries from the right ventricular tract to the lungs, among the infolding pleura of lobes and segments, and along the pulmonary veins back from the lung to the atriums as well as the epicardium on each chambers of the heart needs to be clarified in future studies.

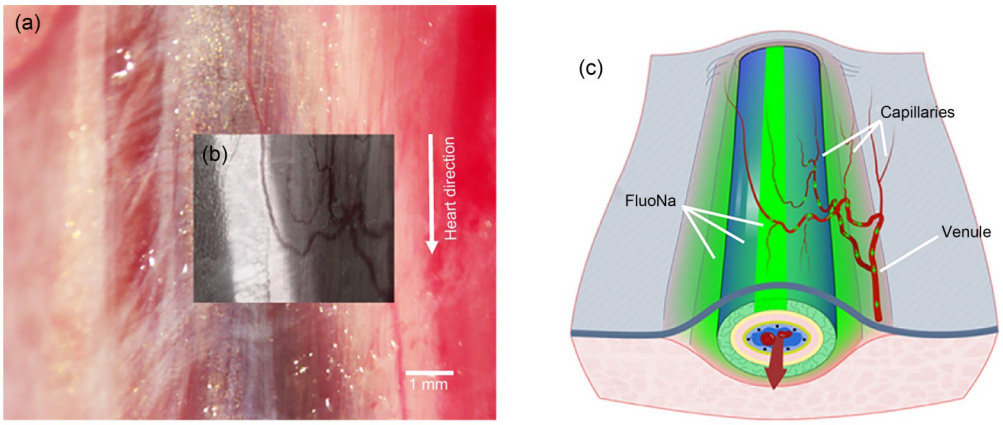

Fig. 7 Interstitial fluid (FluoNa) in a perivascular and adventitial connective tissue (PACT) pathway on a vein entering nearby capillaries. (a) A segment of venous vessel and capillaries (bright-field). (b) A dark-field image of part of (a) and FluoNa in the PACT pathway entering capillaries and a venule nearby (Video S7). (c) A diagram of (a) and (b). (c) The fluorescently stained adventitial interstitial fluid (ISF) flow (green arrows in the capillaries and venules) continuously enters the capillaries and venule along the PACT pathways.

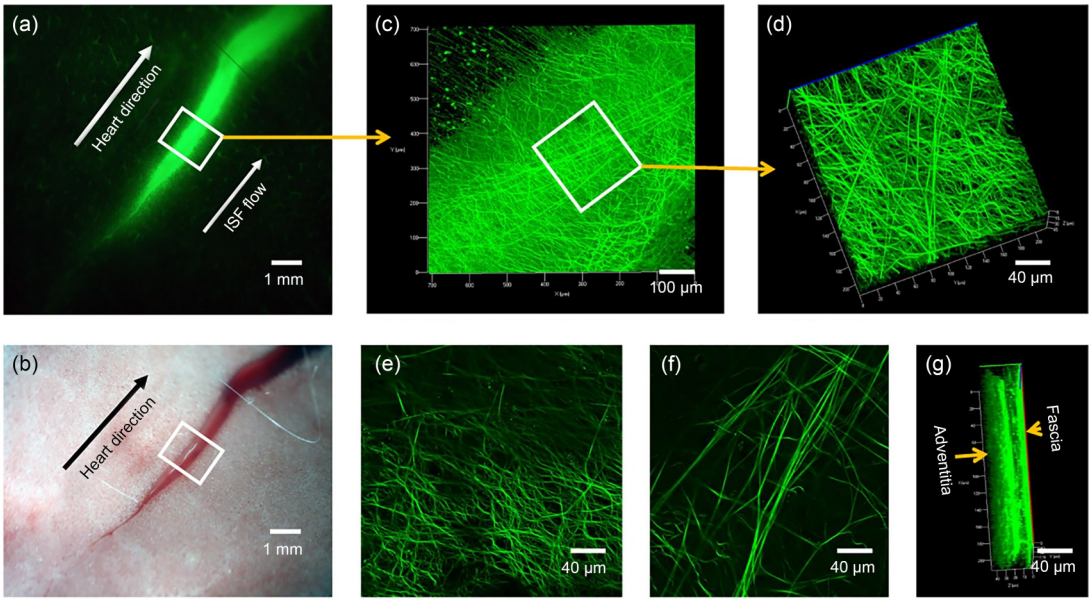

Fig. 8 A segment of pulmonary vein found in the fourth group sacrificed at 15 min after hypodermic injection. (a) A pulmonary vein apparently stained by interstitial fluid (FluoNa) from the ankle dermis. (b) A bright-field image of (a). (c) Two types of fibers on the venous vessel found by confocal laser scanning microscopy (CLSM). (d) A three-dimensional (3D) view of an enlarged image of (c). (e) The cross-linked fibers in the superficial layer of (d) that were stained by FluoNa from the ankle dermis. (f) The longitudinal fibers of adventitia in the deep layer of (d). (g) A side view of (d) showing two layers of stained fibers located in the superficial fascia of the lung and the deep layer of the venous adventitia. The direction of the ISF flow along the pulmonary venous vessel was toward the heart.

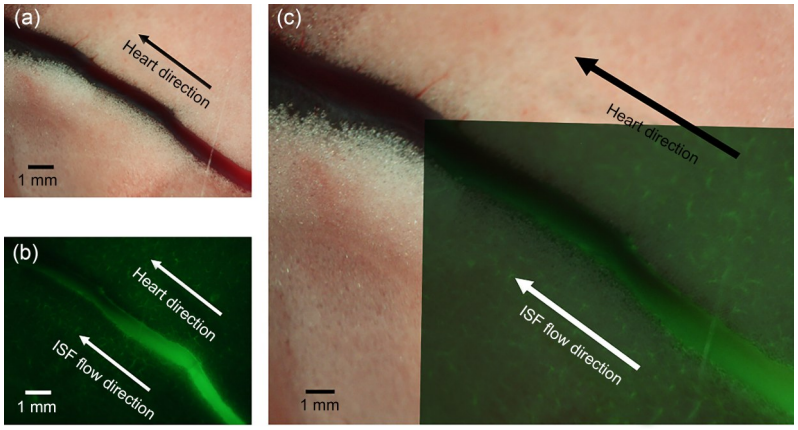

Fig. 9 A segment of pulmonary vein was partially stained by the interstitial fluid (FluoNa) from the legs in a subject of the fourth group. (a) A segment of pulmonary vein on the lung. (b) The distal part of the perivascular and adventitial connective tissue (PACT) pathway on the vein was stained by FluoNa from the legs. (c) Merged image of (a) and (b), which showed the ISF in the PACT pathway on the pulmonary vein flowed toward the heart.

4 Conclusions

In summary, this study revealed more kinetic features of a continuous long-distance ISF flow along blood vessels from the lower limbs to the pericardium, epicardium, and the veins of the lung in an animal. The data revealed a successive process of ISF flow through a PACT pathway, firstly via the adventitia and secondly crossed layers of fascia and into the perivascular connective tissues. When sufficient fluid comes into the PACT pathways, extra fluid would be transported constantly via a smaller space in the adventitia and a bigger space between the covering fascia and the adventitia, and diffuse into the surrounding perivascular connective tissues, like a flow and irrigation system. In the perivascular connective tissues, there might be more types of the continuous ISF flow in layers of fascia, including muscle fascia. The forces driving ISF flow in a long-distance PACT pathway are complicated. For a segmental PACT pathway, "push" and "pull" forces were illustrated. The ability to "pull" ISF flow through long-distance PACT pathways from the limbs to the epicardium depends on at least two factors: a driving source like the mechanically beating heart and a long-distance ISF flow pathway with the intact fibrous framework. The pores of a PACT pathway for ISF flow were not the size of a few molecules, but nano-sized in the adventitia and micron-sized in the space between the adventitia and its covering fascia. When more fluid converges into the PACT pathways, the spaces under layers of fascia might be expanded over micron-meters. Thus, the long-distance PACT pathways for ISF flow were nano-micron-sized in transverse section and macroscopic scale in the longitudinal plane, from the limbs to the heart.

When fluid comes into the PACT pathways, ISF would be continuously transported toward a dynamic driving source or center. We named the space between a solid fiber and the gel-like adventitial matrix, as well as the space between the gel-like adventitia and its covering solid fascia, as an "interfacial zone or interspace." The pattern of ISF flow in a PACT pathway is named as "interfacial fluid flow." When extra actively dynamic driving power is provided, ISF will flow along the solid adventitial fiber or layers of solid fascia rather than diffuse locally. The presented data demonstrated that different types of surfactants played an essential role in ISF flow in a PACT pathway and suggested that there were two parts in the "slit-shaped" PACT pathways: a longitudinal transport channel and an absorptive part for imbibition.

To understand the dynamic mechanism of long-distance ISF flow, the flow dynamics of a "gel pump" was proposed based on the ingenious use of interfacial tension and interactions to regulate ISF flow. The periodic to-and-fro "gel pump" in the heart or lungs is a potential driving force for the systemic ISF flow. In the context of interfacial science, the demonstrated interfacial fluid flow might be another principal fluid dynamic pattern besides convective/vascular and diffusive transport in biological systems. Such interfacial transport pattern represents an actively dynamic capillary

flow phenomena in biological and living systems, the fluid mechanics of which is named as interfacial fluidics. Interfacial fluid flow in diverse tissues or organs might be multiscale, multilayer, and multiform, depending on the shapes of various solid structures. The dynamic mechanisms of different types of interfacial fluid flow regulated by interfacial interactions, interfacial forces, and other driving forces need to be identified respectively. Such a biotic interfacial fluid flow in interstitial connective tissues (named as vegetative or autonomic interstitial fluid system) might provide a physical field between matter phases to transport physical or chemical signals, energy, or information, and regulate physiological functions throughout the whole body by mechanical driving forces and other synergistic dynamic powers. Fluid flow through an arterial PACT pathway will be discussed in other studies. The components conveyed by a PACT pathway need to be verified, but could include fluid, bio-signaling molecules, nutrients, solutes, oxygen, metabolic products, electrical ITZ potential, electromagnetic signals, and drugs.

The cardiovascular system is a sealed conduit network for the rapid convective transport of blood driven by the heart pump. By comparison, a long-distance ISF flow pathway may correspond to a vascular vessel, and a "gel pump" may be equivalent to the heart pump. Unlike in vascular vessels, fluid flow in an ISF pathway contains two patterns: a longitudinal flow (transport channel) toward a driving center and diffusion from the transport channel into the surrounding tissues. By comparison with the indistinct spatial structures that were described by unordered interstitial spaces through the interstitium continuity, a continuous reticular network (Cenaj et al., 2021) or a hierarchical multiphase porous extracellular matrix (Zhu et al., 2019), we suggest that there is an ordered, non-vascular, long-distance, multi-layered, multi-leveled, multi-scaled, multiformed, and topologically connected interfacial space or poly-interspace in the network of fibrous connective tissues throughout the whole body. When fluid enters such spaces, a systemic interfacial fluid flow can be formed, driven mainly by the "gel pumps" of the regular heart beatings and irregular respiratory movements. Moreover, the additional "gel pumps" could be multicentric and be located in diverse organs or tissues, including the intestines, muscles, skin, and nerves. To comprehensively understand the physiological and pathophysiological functions of ISF circulatory networks is an extremely intriguing objective for future studies in life science.

Acknowledgments

This study was supported by the National Natural Science Foundation of China (Nos. 82050004 and 81141118), the Beijing Hospital Clinical Research 121 Project (No. 121-2016002), and the National Basic Research Program of China (No. 2015CB554507). We thank Ms. Siu TUEN, Lucy Chan LAU, Mr. Waichun TIN, and Weiwu HU for their financial support, Prof. Peisu XIA for her help with data analysis, and Prof. Wentai LEE for his assistance with English language corrections to this manuscript.

Author contributions

Hongyi LI conceived the original ideas and concepts, contributed materials, designed the experiments, and wrote the paper. Hongyi LI, Xiaoliang CHEN, and You LYU performed the experiments. Hongyi LI, Qi HUA, Fusui JI, and Hua LI analyzed the data. Hongyi LI and Yajun YIN analyzed the interfacial transport pattern. Hongyi LI and Bei LI prepared pictures and videos. All authors have read and approved the final manuscript and, therefore, have full access to all the data in the study and take responsibility for the integrity and security of the data.

Compliance with ethics guidelines

Hongyi LI, You LYU, Xiaoliang CHEN, Bei LI, Qi HUA, Fusui JI, Yajun YIN, and Hua LI declare that they have no conflict of interest.

All institutional and national guidelines for the care and use of laboratory animals were followed.

References

Aukland K, Reed RK, 1993. Interstitial-lymphatic mechanisms in the control of extracellular fluid volume. *Physiol Rev*, 73(1):1-78. https://doi.org/10.1152/physrev.1993.73.1.1

Cenaj O, Allison DHR, Imam R, et al., 2021. Evidence for continuity of interstitial spaces across tissue and organ boundaries in humans. *Commun Biol*, 4:436. https://doi.org/10.1038/s42003-021-01962-0

Chen X, Cao GX, Han AJ, et al., 2008. Nanoscale fluid transport: size and rate effects. *Nano Lett*, 8(9):2988-2992. https://doi.org/10.1021/nl802046b

Hall JE, Guyton AC, 2011. The microcirculation and lymphatic system. *In*: Guyton and Hall Textbook of Medical Physiology, 12th Ed. Saunders, Philadelphia, p.180-182.

Holmberg K, Jönsson B, Kronberg B, et al., 2003. Surfactants and Polymers in Aqueous Solution, 2nd Ed. John Wiley & Sons, Chichester, UK, p.139-155. https://doi.org/10.1002/0470856424.ch6

Holmes MC, 1998. Intermediate phases of surfactant-water mixtures. *Curr Opin Colloid Interface Sci*, 3(5):485-492.

https://doi.org/10.1016/S1359-0294(98)80022-8

Iliff JJ, Wang MH, Liao YH, et al., 2012. A paravascular pathway facilitates CSF flow through the brain parenchyma and the clearance of interstitial solutes, including amyloid β. *Sci Transl Med*, 4(147):147ra111. https://doi.org/10.1126/scitranslmed.3003748

Khan A, 1996. Phase science of surfactants. *Curr Opin Colloid Interface Sci*, 1(5):614-623. https://doi.org/10.1016/S1359-0294(96)80099-9

Levick JR, 1987. Flow through interstitium and other fibrous matrices. *Q J Exp Physiol*, 72(4):409-437. https://doi.org/10.1113/expphysiol.1987.sp003085

Li HY, Chen M, Yang JF, et al., 2012. Fluid flow along venous adventitia in rabbits: is it a potential drainage system complementary to vascular circulations? *PLoS ONE*, 7(7): e41395. https://doi.org/10.1371/journal.pone.0041395

Li HY, Yang CQ, Lu KY, et al., 2016. A long-distance fluid transport pathway within fibrous connective tissues in patients with ankle edema. *Clin Hemorheol Microcirc*, 63(4):411-421. https://doi.org/10.3233/CH-162057

Li HY, Han D, Li H, et al., 2017. A biotic interfacial fluid transport phenomenon in the meshwork of fibrous connective tissues over the whole body. *Prog Physiol Sci*, 48(2):81-87 (in Chinese). https://doi.org/10.3969/j.issn.0559-7765.2017.02.001

Li HY, Yang CQ, Yin YJ, et al., 2019. An extravascular fluid transport system based on structural framework of fibrous connective tissues in human body. *Cell Prolif*, 52(5): e12667. https://doi.org/10.1111/cpr.12667

Li HY, Yin YJ, Yang CQ, et al., 2020. Active interfacial dynamic transport of fluid in a network of fibrous connective tissues throughout the whole body. *Cell Prolif*, 53(2):e12760. https://doi.org/10.1111/cpr.12760

Pan H, Wang BH, Li ZB, et al., 2019. Mitochondrial superoxide anions induced by exogenous oxidative stress determine tumor cell fate: an individual cell-based study. *J Zhejiang Univ-Sci B (Biomed & Biotechnol)*, 20(4):310-321. https://doi.org/10.1631/jzus.B1800319

Qian M, Niu LL, Wang YP, et al., 2010. Measurement of flow velocity fields in small vessel-mimic phantoms and vessels of small animals using micro ultrasonic particle image velocimetry (micro-EPIV). *Phys Med Biol*, 55(20): 6069-6088. https://doi.org/10.1088/0031-9155/55/20/003

Rennels ML, Gregory TF, Blaumanis OR, et al., 1985. Evidence for a 'Paravascular' fluid circulation in the mammalian central nervous system, provided by the rapid distribution of tracer protein throughout the brain from the subarachnoid space. *Brain Res*, 326(1):47-63. https://doi.org/10.1016/0006-8993(85)91383-6

Tokunaga TK, Wan JM, 1997. Water film flow along fracture surfaces of porous rock. *Water Resour Res*, 33(6):1287-1295. https://doi.org/10.1029/97WR00473

Tuller M, Or D, Dudley LM, 1999. Adsorption and capillary condensation in porous media: liquid retention and interfacial configurations in angular pores. *Water Resour Res*, 35(7):1949-1964. https://doi.org/10.1029/1999WR900098

van Oss CJ, 2007. Development and applications of the interfacial tension between water and organic or biological surfaces. *Colloids Surf B: Biointerfaces*, 54(1):2-9. https://doi.org/10.1016/j.colsurfb.2006.05.024

Whitby M, Cagnon L, Thanou M, et al., 2008. Enhanced fluid flow through nanoscale carbon pipes. *Nano Lett*, 8(9): 2632-2637. https://doi.org/10.1021/nl080705f

Wiig H, Rubin K, Reed RK, 2003. New and active role of the interstitium in control of interstitial fluid pressure: potential therapeutic consequences. *Acta Anaesthesiol Scand*, 47(2):111-121. https://doi.org/10.1034/j.1399-6576.2003.00050.x

Wiig H, Gyenge CC, Tenstad O, 2005. The interstitial distribution of macromolecules in rat tumours is influenced by the negatively charged matrix components. *J Physiol*, 567(2):557-567. https://doi.org/10.1113/jphysiol.2005.089615

Ziemys A, Kojic M, Milosevic M, et al., 2012. Interfacial effects on nanoconfined diffusive mass transport regimes. *Phys Rev Lett*, 108(23):236102. https://doi.org/10.1103/PhysRevLett.108.236102

Zhu Y, Zhang Q, Shi X, et al., 2019. Hierarchical hydrogel composite interfaces with robust mechanical properties for biomedical applications. *Adv Mater*, 31(45):1804950. https://doi.org/10.1002/adma.201804950

Supplementary information

Videos S1–S7